

# Lattice models for ballistic aggregation in one-dimension

SUPRAVAT DEY<sup>1</sup>, DIBYENDU DAS<sup>1</sup> and R. RAJESH<sup>2</sup>

<sup>1</sup> *Department of Physics, Indian Institute of Technology Bombay, Powai, Mumbai-400076, India*

<sup>2</sup> *Institute of Mathematical Sciences, CIT campus, Taramani, Chennai-600113, India*

PACS 45.70.-n – Granular systems

PACS 47.70.Nd – Nonequilibrium gas dynamics

PACS 05.40.-a – Fluctuation phenomena, random processes, noise, and Brownian motion

**Abstract.** - We propose two lattice models in one dimension, with stochastically hopping particles which aggregate on contact. The hops are guided by “velocity rates” which themselves evolve according to the rules of ballistic aggregation as in a sticky gas in continuum. Our lattice models have both velocity and density fields and an appropriate real time evolution, such that they can be compared directly with event driven molecular dynamics (MD) results for the sticky gas. We demonstrate numerically that the long time and large distance behavior of the lattice models are identical to that of the MD, and some exact results known for the sticky gas. In particular, the exactly predicted form of the non-Gaussian tail of the velocity distribution function is clearly exhibited. This correspondence of the lattice models and the sticky gas in continuum is nontrivial, as the latter has a deterministic dynamics with local kinematic constraint, in contrast with the former; yet the spatial velocity profiles (with shocks) of the lattice models and the MD have striking match.

**Introduction.** – A gas of ballistically moving particles which suffer completely inelastic collisions amongst themselves and thereby aggregate, is well known as the *sticky* gas. The motion of the particles are deterministic and the collisions follow the momentum and mass conservation laws. The problem becomes statistical as the initial velocities of the particles are assumed to be random. The system exhibits large scale density clustering with a growing coarsening length scale, and appearance of shocks in spatial velocity profile. The connection between this problem and shock dynamics of a Burgers fluid in the high Reynolds number limit was established in [1]. The sticky gas problem has some relevance for interstellar matter, as similarities between self gravitating matter and inertial Burgers fluid was shown in [2]. In the context of terrestrial dissipative granular matter, a mean field analysis of the model with several scaling predictions was introduced in [3]. The model was exactly solved for several statistical functions in [4, 5].

*A priori* the sticky gas, which is a gas of particles with zero restitution coefficient ( $r$ ) may appear to be rather artificial, since real granular gases all have  $0 < r < 1$ . In fact in reality,  $r$  is also dependent on the relative velocity  $v_{\text{rel}}$  of collisional impact — for the  $v_{\text{rel}} \rightarrow 0$ ,  $r \rightarrow 1$  [6, 7]. Very interestingly it has been shown that for intermediate

times (but not very large [8]) such a realistic granular gas with any  $r$  ( $0 < r < 1$ ) behaves statistically similarly as a sticky gas ( $r = 0$ ) [9, 10]. This remarkable universality, hitherto is only supported by molecular dynamics (MD) and not proved analytically. In particular, since the mapping between the particle-dynamics of the sticky gas and shock-dynamics of the Burgers fluid is known [1] and several properties of the sticky gas and the Burgers equation has been derived analytically [4, 5, 11], one hopes that the speculation of the inviscid Burgers equation being the correct continuum limit of the finite  $r$  granular gas should be analytically provable.

In certain non-equilibrium problems like diffusion limited reactions [12–14], a quantum field theoretic formalism has been develop to systematically connect the stochastic dynamics of appropriate lattice models to their respective continuum Langevin dynamical limits. Motivated by the latter works we wonder if a similar method can be followed for the granular gas problem discussed above. Can one invent suitable stochastic lattice models which may represent the microscopic ballistic granular gas problem? The proposal is rather ambitious for  $r \neq 0$ , but one may start with the simpler sticky gas (i.e. the  $r = 0$  case). In this paper, we propose two stochastic lattice models (with single and multi-particle occupancies per site respectively)

which are shown to have the same statistical properties, at long times and large distances, as the sticky gas. Statistical distribution functions of the mass and velocity, spatial density-density correlation functions, and velocity shock profiles, for our lattice models are shown to have striking match with exact results and MD simulation results of the sticky gas. Of the two models we discuss below, the single particle occupancy model would seem a natural counterpart of the sticky gas. On the other hand, the second model with multiple site occupancy and a delayed aggregation would a priori seem a bit different — although in the limit of a tuning parameter we show that it reduces to the single occupancy model. Explicit study of a multiple particle occupancy model is motivated by the fact that the field theoretic literature [12, 13] have generally dealt with multiple occupancy models. Furthermore they are also natural for future extension of our study to the  $r \neq 0$  case, where particles do not stick after collisions. Thus our choice of the models leave open the scope of coarse graining in future, and obtaining the desired continuum limit.

Although lattice models have been studied earlier [15–19] for the freely cooling granular gas, to understand the velocity ordering and formation of spatial shocks they had many limitations. Firstly, these earlier models only had lattice velocities which evolved stochastically and they involved no actual particles hopping. As a result although key insights on the behavior of the velocity field could be obtained, the “density field” could not be tracked. Moreover the time used for characterizing evolution of the system was “collision number”, and matching to real time evolving MD involved arbitrariness. Finally kinematic rules had to be specified separately on the lattice models to avoid collisions disallowed by the ballistic dynamics. In the models that we present in this paper, these shortcomings have been overcome. We have actual particles hopping and so both the velocity and mass density fields can be tracked. The time evolution is done using prescriptions of exact stochastic simulation of Master equation, such that it compares directly with time in MD simulations. Interestingly the stochastic dynamics in our models naturally take care of one type of kinematically forbidden collisions, but violates another type (a slower particle can catch up with a faster one from behind). In spite of this lack of strict adherence to kinematic constraints we show that the results of velocity shock profiles are nevertheless almost identical to MD for identical initial conditions. Thus we claim our lattice models to be minimally complex models necessary to represent the sticky gas system, and may hope (as discussed above) that in future they may be appropriately coarse-grained to derive the inviscid Burgers equation.

Below we begin by first defining the single and multiple occupancy lattice models SOSG and MOSG, respectively.

**Model I: Single occupancy sticky gas (SOSG).** — The system has massive particles on a one-dimensional

periodic lattice of size  $L$ . An occupied site  $i$  at time  $t$  (where  $i$  can take values  $1, 2, \dots, L$ ) has two non-zero variables: mass  $m_i$  and “velocity”  $v_i$ . The magnitude of the velocity  $v_i$  specifies the rate of hopping of the particle to its nearest neighbors, and its sign decides the direction of hopping. For an unoccupied site we designate  $m_i = 0$  and  $v_i = 0$ . We initialize the system by having  $m_i = 1 \forall i$  and assigning random velocities  $v_i$  drawn from a uniform box distribution over the range  $(-1, +1)$ . The system evolves in time via hopping and instantaneous aggregation events. Let the sites  $i$  and its neighbor  $j$  have variables  $(m_i, v_i)$  and  $(m_j, v_j)$  respectively at time  $t$ . The particle of the site  $i$  may hop to either of its neighbors  $j (= i + 1, i - 1)$  depending on  $\text{sgn}(v_i) (= +1, -1)$ , and with the rate  $|v_i|$ . If at time  $t + \delta t$  the particle at the  $i^{\text{th}}$  actually hops to the  $j$  then the masses and the velocities change in the following way:  $m_i \rightarrow 0$ ,  $v_i \rightarrow 0$ ,  $m_j \rightarrow m_i + m_j$ , and  $v_j \rightarrow (m_i v_i + m_j v_j) / (m_i + m_j)$ . The latter update of  $v_j$  follows the momentum conservation rule of particle collision with zero restitution coefficient.

To implement the above dynamics, in our stochastic simulation, we choose an event of hopping of a particle at site  $i$  with probability  $|v_i| / \Gamma$  [20–23], where  $\Gamma = \sum_i |v_i|$  is the sum of all hopping rates possible in the system at the time  $t$ . The enactment of the event is associated with a time increment  $\delta t$ , which we choose to be the reciprocal of the total rate  $\Gamma$ , i.e  $\delta t = 1 / \Gamma$ . As  $\Gamma$  is time dependent in this problem,  $\delta t$  is also time dependent. We note that this choice of  $\delta t$  is the average value of the truly random  $\delta t$  drawn from its distribution function  $\Gamma \exp(-\Gamma \delta t)$  [20–23]. Although using a random  $\delta t$  would have been more appropriate in principle, for very small rate  $\Gamma$  as we have at large times, sampling its full distribution becomes very tedious numerically. Using instead the average value  $\delta t = 1 / \Gamma$  saves numerical effort considerably, without compromising accuracy (as we have checked).

**Model II: Multiple occupancy sticky gas (MOSG).** — In this model we also have a system of massive particles on an one-dimensional periodic lattice of  $L$  sites, except that now multiple particles can occupy any site. For a site  $i$  occupied by  $\alpha^{\text{th}}$  particle, we associate two variables  $m_{i,\alpha}$  and  $v_{i,\alpha}$ . If the number of particles at site  $i$  is  $n_i$ , then  $\alpha$  can take values  $1, 2, \dots, n_i$ . As in SOSG  $|v_{i,\alpha}|$  denotes the rate of hopping while  $\text{sgn}(v_{i,\alpha}) (= +1, -1)$  decides to which neighboring site  $j = (i + 1, i - 1)$  the particle may hop. The system evolves via hopping followed by aggregation, except that in MOSG unlike SOSG, aggregation events are not instantaneous. At any site  $i$ , a pair of particles  $\alpha$  and  $\beta$  may aggregate with a rate  $\lambda$ . In the limit of  $\lambda \rightarrow \infty$ , aggregation events becomes instantaneous leading to maximum occupancy of the sites being 1 — thus MOSG maps back to SOSG. We initialize the system by having  $n_i = 1$  and  $m_{i,\alpha} = 1 \forall i$ , and assigning random velocities  $v_{i,\alpha}$  drawn from a uniform box distribution over the range  $(-1, +1)$ . After aggregation of two particles  $\alpha$  and  $\beta$  at site  $i$ ,  $m_{i,\alpha} \rightarrow m_{i,\alpha} + m_{i,\beta}$ ,

$v_{i,\alpha} \rightarrow (m_{i,\alpha}v_{i,\alpha} + m_{i,\beta}v_{i,\beta}) / (m_{i,\alpha} + m_{i,\beta})$ , and  $n_i \rightarrow n_i - 1$ .

As in SOSG the stochastic simulation is implemented by choosing events of hopping of particles and their aggregation randomly with probabilities  $|v_{i,\alpha}|/\Gamma$  and  $\lambda/\Gamma$  respectively. Here  $\Gamma = \sum_{i,\alpha} |v_{i,\alpha}| + \sum_i n_i(n_i - 1)\lambda/2$  is the sum of all hopping and aggregation rates possible in the system at the time  $t$ . Note that the factor  $n_i(n_i - 1)/2$  comes from the number of possible collisions among any pair of particles at site  $i$ . The increment of time between two events is chosen to be  $\delta t = 1/\Gamma$ .

As noted above, both the models SOSG and MOSG are more realistic in having on one hand both local mass density and velocity fields, and on the other hand realistic time increments  $\delta t$ . In both these respects we overcome serious drawbacks of the earlier lattice models [15–17, 19] of dissipative gases in making contact with molecular dynamics and continuum theories. At the same time the models being stochastic and not having strict kinematic constraint (as will be discussed below), leave the curious question open as to whether their long time and large wavelength properties would match with that of the deterministically evolving ballistic aggregation model. We now proceed to show numerically that such a non-trivial correspondence is indeed exhibited by both the models.

**Results.** – For both SOSG and MOSG lattice models we use system sizes  $L = 50000$ . As mentioned before the hopping rates  $v_i$  (in SOSG) and  $v_{i,\alpha}$  (in MOSG) are initially chosen to be random and drawn from the uniform box distribution over range  $(-1,1)$ . In MOSG we have used the aggregation rate  $\lambda = 5.0$ . The unit of time  $t$  in our lattice simulations is inverse of the unit of rates — as rates are chosen to be dimensionless, the time is also dimensionless. Similarly the space  $x$  in units of the lattice spacing is taken as dimensionless.

The choice of the value of  $\lambda = 5.0$  is based on the observation of energy decay in MOSG for various values of  $\lambda$  shown in Fig. 1. The scaled energy  $e(t)$  for the MOSG model with different  $\lambda$ , tend to that of the SOSG model for increasing  $\lambda$ . For large  $t$  both the models follow the classic energy decay  $e(t) \sim t^{-2/3}$  [3, 5, 9] well known for the ballistic sticky gas. In particular for  $\lambda = 5.0$  we can see from Fig. 1 that for times  $t \geq 10^2$  the MOSG and SOSG curves are completely merge, implying that we are safely in the universal sticky gas regime. Interestingly the irrelevance of  $\lambda$  and the universality of  $e(t)$  at large  $t$ , is reminiscent of a similar irrelevance of the values of restitution coefficient in connection to energy decay of granular gases in one-dimension [9].

Exact analytical results in terms of explicit functions and integrals for the mass and velocity distribution functions of the sticky gas are available [4, 5]. On the other hand the mass density-density spatial correlation function, although not available as an explicit analytic form, can easily be obtained from event driven molecular dynamics (MD) simulation of the sticky gas [10]. Below we first proceed to match the numerically obtained mass and velocity

distributions from the SOSG and MOSG models with the exact analytical results. Then we compare the mass density correlator of SOSG and MOSG models with that of MD. Finally, even the microscopic spatial velocity shock profile of the two lattice models are shown to be almost identical to that of the MD.

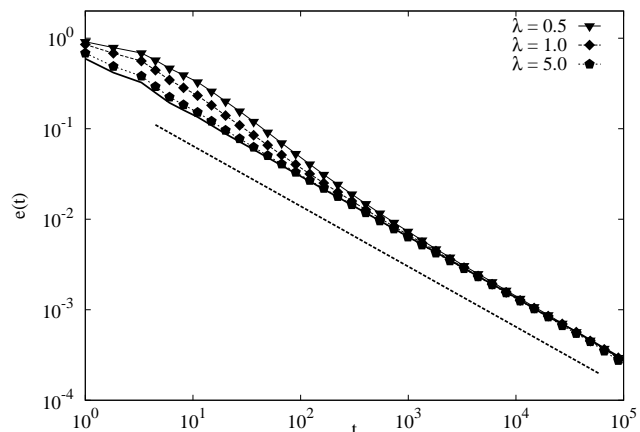


Fig. 1: Log-log plot of Energy  $e(t) = E(t)/E_0$  with time  $t$ , where  $E(t)$  is the total energy at time  $t$  and  $E_0 = E(t = 0)$ . Data points with lines joining them are for the MOSG model with different values of  $\lambda$  indicated as labels. The solid line is for the SOSG model. The dashed line has slope  $-2/3$  and serves as a guide to eye.

*Comparison of the lattice model results with the analytical results.* The exact analytical solution of the sticky gas problem [4, 5] relies on reducing the calculation of the distribution functions to a summing of Brownian paths with parabolic constrains in momentum space. The diffusion constant  $D$  associated with the effective Brownian motion is exactly equal to the inverse of the variance  $\beta$  of the initial momentum distribution of the particles in the sticky gas [5]. The following distribution functions for the scaled mass  $M = m/t^{2/3}$  and scaled velocity  $V = vt^{1/3}$  were derived in [5] as follows:

$$\mu_1(M) = \beta M \mathcal{I}(M) \mathcal{H}(M) \quad (1)$$

$$\bar{\mu}_1(V) = 2 \left( \frac{\beta}{2} \right)^{4/3} \int_0^\infty dM M \mathcal{I}(M) \times \mathcal{J}(V - M/2) \mathcal{J}(-V - M/2) \quad (2)$$

where,

$$\begin{aligned} \mathcal{H}(M) &= \frac{1}{2i\pi} \int_{-i\infty}^{+i\infty} dw \frac{e^{-(\frac{\beta}{2})^{1/3} M w}}{\text{Ai}^2(w)} \\ \mathcal{I}(M) &= \sum_{k \geq 1} e^{-(\frac{\beta}{2})^{1/3} \omega_k M} \\ \mathcal{J}(Y) &= \frac{1}{2i\pi} \int_{-i\infty}^{+i\infty} dw \frac{e^{(\frac{\beta}{2})^{1/3} Y w}}{\text{Ai}(w)}. \end{aligned} \quad (3)$$

In Eq. 3  $\text{Ai}$  is the Airy function [24] and  $-\omega_k$  ( $k=1,2,3,\dots$ ) are its zeros.

The only parameter appearing Eqs. 1, 2, and 3 is  $\beta$  which has to be fixed to match these formulas with our simulation results. In both the lattice models the initial mass of every particle is unity, and hence the variance of the momentum distribution is same as that of the velocity distribution. The variance of the uniform box distribution of velocities over the range  $(-1,1)$  is  $\beta = 1/3$ . Using the latter value of  $\beta$ , we evaluate the integrals  $\mathcal{H}$  and  $\mathcal{J}$  using the “quadgk” function with absolute tolerance =  $10^{-14}$  in MATLAB. The evaluation of the sum  $\mathcal{I}(M)$  was done using our own code — for large  $M$  ( $M \geq 0.1$ ) we kept up to 6000 terms in the sum, while for small  $M$  ( $M < 0.1$ ) we used the asymptotic formula  $\mathcal{I}(M) \simeq 1/\sqrt{2\pi\beta M^3}$  [5].

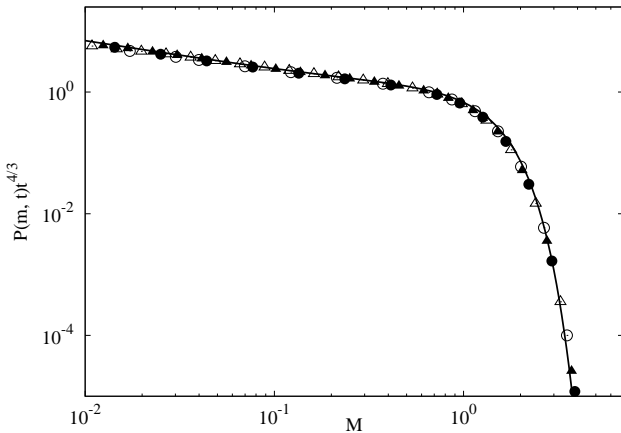


Fig. 2: Log–log plot of  $P(m,t)t^{4/3}$  versus  $M = m/t^{2/3}$  for two different models at two different times. Circular symbols ( $\circ$ ,  $\bullet$ ) represent the SOSG data, while triangular symbols ( $\triangle$ ,  $\blacktriangle$ ) represent the MOSG data. Empty symbols are data for  $t = 8 \times 10^3$  and solid symbols are data for  $t = 16 \times 10^3$ . The solid line is the exact analytical formula of Eq. 1.

The mass distribution function  $P(m,t)$  is related to the scaling function  $\mu_1(M)$  (Eq. 1) as follows:

$$P(m,t) = \frac{1}{t^{4/3}} \mu_1(M). \quad (4)$$

In the simulation of the SOSG model at any given time  $t$ , we drew the frequencies of the non-zero integer masses sweeping over all the sites of the lattice. In contrast, in the MOSG model the frequencies of the total mass ( $\sum_{\alpha=1}^{n_i} m_{i,\alpha}$ ) of every occupied site were drawn, again sweeping over the lattice sites. Normalizing the frequencies by  $L$  and averaging these further over several random initial conditions ( $\sim 10^4$ ) we finally obtained the mass distribution function  $P(m,t)$ . The latter distribution functions obtained for the stochastic SOSG and MOSG models at two different times namely  $t = 8 \times 10^3$  and  $t = 16 \times 10^3$  are scaled (Eq. 4) and plotted in Fig. 2. The exact scaling function  $\mu_1(M)$  enumerated by the method described above is plotted against the data of the lattice models. The spectacular match of the Monte Carlo data and the exact formula, without any parameter fitting, gives the

first evidence to our claim that the lattice models SOSG and MOSG are correct representatives of the continuum behavior of the sticky gas.

We now proceed to look at the velocity distributions for the lattice models. The normalized distribution of our interest scales as follows:

$$Q(v,t) = t^{1/3} f_1(vt^{1/3}), \quad (5)$$

where  $f_1(V) = \bar{\mu}_1(V)/\int_{-\infty}^{\infty} \bar{\mu}_1(V)$ , and  $\bar{\mu}_1(V)$  is given by Eq. 2. Unlike the integer masses  $m$ , the velocities are real numbers, so a numerical binning is required to obtain a distribution function. For SOSG, at any time  $t$  we find the frequencies of velocities of occupied sites falling within coarse-grained bin widths of magnitude 0.001. For MOSG, the frequencies of average velocities ( $\sum_{\alpha=1}^{n_i} v_{i,\alpha}/n_i$ ) of occupied sites falling within different bins (each of width = 0.001) were obtained. We normalize these frequencies by the total number of occupied sites and the bin width. Since the tail of the velocity distribution is of great interest, to obtain high precision, we had to average over relatively much larger set of initial conditions in this case (namely  $\sim 10^7$ ).

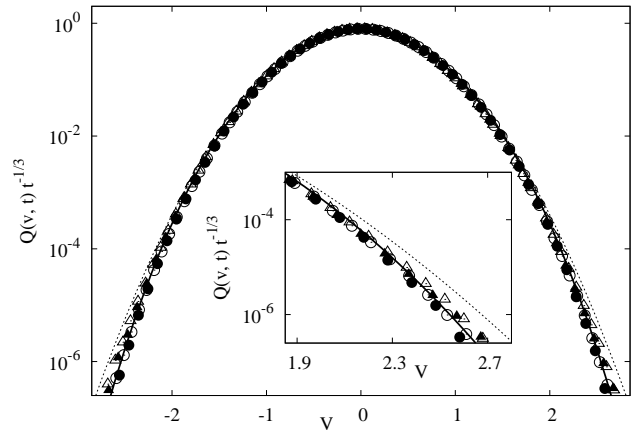


Fig. 3: Log–linear plot of  $Q(v,t)/t^{1/3}$  versus  $V = vt^{1/3}$  for two different models at two different times. Circular symbols ( $\circ$ ,  $\bullet$ ) represent the SOSG data, while triangular symbols ( $\triangle$ ,  $\blacktriangle$ ) represent the MOSG data. Empty symbols are data for  $t = 8 \times 10^3$  and solid symbols are data for  $t = 16 \times 10^3$ . The solid line is the  $f_1(V)$  using exact analytical formula for  $\bar{\mu}_1(V)$  (Eq. 2). The dotted line is a Gaussian curve with zero mean and variance = 0.26 which fits only the small  $V$  data. Inset: A zoom into the tail region of  $Q(v,t)/t^{1/3}$  versus  $V$  (for positive  $V$ ) to show clearly the deviation of the data and the exact formula from the Gaussian form.

The velocity distribution data obtained from the lattice models SOSG and MOSG at two different times namely  $t = 8 \times 10^3$  and  $t = 16 \times 10^3$  are scaled (Eq. 5) and plotted in Fig. 3. The exact curve of  $f_1(V)$  (obtained using  $\bar{\mu}_1(V)$  of Eq. 2) shown with a solid line in Fig. 3 passes all the way through the Monte Carlo data. Again the spectacular match of the data and the exact result without any parameter fiddling is to be noted. A Gaussian

curve shown in dotted line fits the data for small  $V$ , but the tails of the data depart from it.

The asymptotic form of the Eq. 2 for large  $V$ , i.e. the tail, is not known exactly. In [5] the tail was shown to be bounded as  $\bar{\mu}_1(V \rightarrow \infty) \leq \text{constant } |V| \exp(-\beta|V|^3/6 - (\beta/2)^{1/3}|V|\omega_1)$ . The inset of Fig. 3 shows the Monte Carlo data near the tail; the deviation from Gaussianity and match with the exact Eq. 2 are conclusive. However, to determine the precise asymptotic decay, we will require data for much larger range of  $V$ . At this point we would like to recall that finding non-Gaussianity in numerical study of freely cooling granular gases has been an extremely challenging task in earlier works. For example in one-dimensional granular gas with finite restitution coefficient [9], although the system was argued to approach the sticky gas limit asymptotically, the numerical data for the velocity distribution did not clearly show deviation from Gaussianity. We have checked that the computation time involved in MD is very huge to attain the necessary accuracy to demonstrate the deviation of the tail of the distribution from the Gaussian form. Interestingly in a very different context of quasi-elastic limit of granular gas, ‘stationary’ velocity distribution with tail of the form  $\exp(-c|V|^3)$  have been numerically demonstrated [25] but that does not directly address the concerned limit ( $r = 0$ ) of this paper. Given this background it is significant that we have succeeded in demonstrating the deviation from Gaussianity of the tail of the velocity distribution with comparative ease in the Monte Carlo simulations of the lattice models SOSG and MOSG.

#### Comparison of the lattice model results with MD results.

Event driven MD of ballistically moving sticky particles in continuum is expected to yield numerically exact results, if done with sufficient accuracy. The details of such simulation can be found in a recent publication [10]. Here we use event driven MD to study the spatial mass density-density correlation function and spatial velocity profile, compare these with that obtained from Monte-Carlo simulation of the SOSG and MOSG models.

The local mass density function is defined in the following fashion. For the SOSG and MOSG models a local site mass density  $m_i$  is defined as the total mass at site  $i$ . For the MD simulation the whole continuum space of length  $L$  is divided into  $L$  boxes and the sum total of masses in the  $i^{\text{th}}$  box denotes the mass density  $m_i$  of the box [10]. The density-density correlation function  $C_{mm}(x, t) = \langle m_i(t)m_{i+x}(t) \rangle$ . Here, the angular bracket  $\langle \cdot \rangle$  represents average over both space ( $i$ ) and initial velocities, in all the three systems. In MD simulations with  $L$  particles, the system is initialized to have random particle velocities drawn from an uniform box distribution over  $(-1, 1)$ , and unit particle masses kept at unit separations. In MD too we use  $L = 50000$ . Thus the initial conditions are same for MD and the two lattice models, although their subsequent dynamics are very different.

The mass density-density correlation functions are

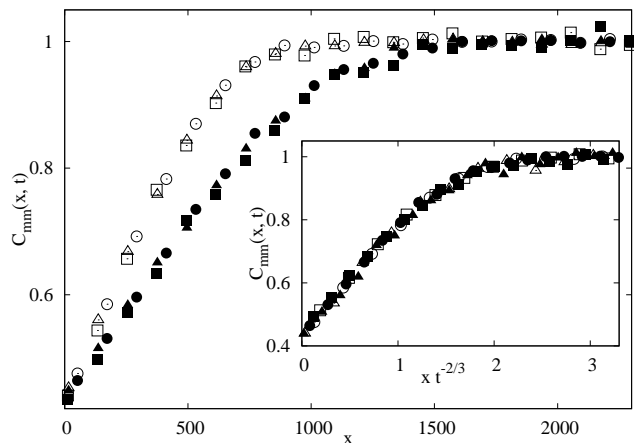


Fig. 4: Plot of  $C_{mm}(x, t)$  versus  $x$  for the MD simulations and the two different lattice models, at two different times. Empty symbols are data for  $t = 8 \times 10^3$  and solid symbols are data for  $t = 16 \times 10^3$ . Circular symbols ( $\circ$ ,  $\bullet$ ) represent the SOSG data, triangular symbols ( $\triangle$ ,  $\blacktriangle$ ) represent the MOSG data, and the square symbols ( $\square$ ,  $\blacksquare$ ) represent the MD data. Inset shows plot of  $C_{mm}(x, t)$  versus  $x/\mathcal{L}(t)$  for the six curves in the main figure — the data collapse according to Eq. 6.

shown in Fig. 4 at two different times. At both the time instants the data of the lattice models and the MD simulations fall perfectly on top of each other, without any parameter fixing. The profile of the correlation function is characteristic of the sticky gas and has been discussed in [10]. As the system coarsens in time,  $C_{mm}(x, t)$  is expected to obey the scaling hypothesis [26] when space is scaled with the coarsening length  $\mathcal{L}(t) \sim t^{2/3}$ :

$$C_{mm}(x, t) = g\left(\frac{x}{\mathcal{L}(t)}\right). \quad (6)$$

As shown in the inset of the Fig. 4, there is perfect data collapse following the above equation.

Unlike spatial correlation functions which capture ordering and structure formation at the macroscopic level, microscopic information is captured by the spatial velocity profile of a sticky gas. The velocity profile  $v(x)$  exhibit shocks joined by approximate linear curves [1, 9, 19]. In Fig. 5 we show particle-velocity  $v(x)$  versus  $x$  for the MD simulation with visible shocks (where velocity jumps suddenly from positive to negative) as expected. It is remarkable that for the SOSG and the MOSG lattice models the velocity profile of occupied site at the same time  $t$ , are almost identical as the MD (Fig. 5) provided their initial conditions are identical. Although in an earlier work such a correspondence was demonstrated [19], there the shocks in the velocity profile had an inverse correspondence to the shocks in MD — lattice shocks were located at positions where MD profile was gradual and vice versa; this was a consequence of the fact that there were no actual motion of particles along the lattice. Contrary to that since we have actual particles hopping on lattice, we have natural and direct correspondence of shock profiles with the MD

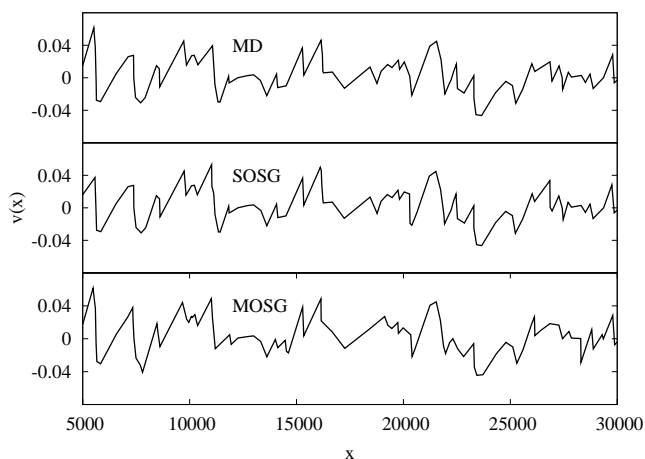


Fig. 5: Velocity profiles  $v(x)$  plotted against space  $x$  (which is continuous for MD and assumes integer values for the SOSG and MOSG models). The profiles of  $v(x)$  at time  $t = 10^4$  look almost identical in the three cases, for the same initial realization of random velocities.

(Fig. 5). Moreover it was emphasized in [19] that local kinematic constraints had to be separately imposed on the lattice dynamics to ensure that collisions disallowed by the ballistic dynamics do not occur, and this was argued to be a key factor for shock formation. The kinematic constraint states that if  $v_R - v_L > 0$  (where  $v_L$  and  $v_R$  denote velocities of a pair of left and right particles, respectively) collisions won't occur. The collisions disallowed by the latter rule can be classified into two types: (a)  $v_R > 0$  and  $v_L < 0$ , (b)  $v_R > v_L$  with same sign for both. In our simulation since hopping in the opposite direction of rate  $v$  is disallowed, case (a) is automatically taken care of — this we would claim is indeed the key condition for shock formation. On the other hand, due to the stochastic nature of hopping in our models, constraint (b) is sometimes violated (a slower particle may catch up with a faster one) — yet the latter violation has no discernible effect (Fig. 5) on the microscopic shock profile. Hence we conclude that constraint (b) is not an essential constraint.

**Discussion.** — We have shown that two lattice models with single and multiple particles site occupancy and stochastic dynamics, can exactly reproduce the long time and large space behavior of the ballistic sticky gas system. In particular, the mass and velocity distribution functions are identical to the exact analytically known distributions of the sticky gas. The density-density spatial correlation functions and local microscopic velocity shock profiles of the lattice models and MD simulations also have a perfect match.

As we have noted that the current lattice models differ from earlier lattice models in having a genuine density field besides the velocity field. The time update is done following a prescription suited for real continuous time evolution, allowing us to directly compare our results with

exact analytical and MD simulation results. The lattice dynamics violates the strict conditions of kinematic constraint, but only mildly, so that there is no observable effect over slightly coarse-grained spatial scale (see Fig. 5).

Based on the results that we have found, a curious possibility has been opened up to derive the continuum behavior of the granular gases in future. We hope that the two lattice models studied here have all the necessary ingredients sufficient to capture the correct continuum behavior of the sticky gas; the models should lead to the inviscid Burgers equation if they can be successfully coarse grained by a suitable technique.

## REFERENCES

- [1] KIDA S., *J. Fluid. Mech.* , **93** (1979) 337.
- [2] SHANDARIN S. F. and ZELDOVICH Y. B., *Rev. Mod. Phys.* , **61** (1989) 185.
- [3] CARNEVALE G. F., POMEAU Y. and YOUNG W. R., *Phys. Rev. Lett.* , **64** (1990) 1913.
- [4] FRACHEBOURG L., *Phys. Rev. Lett.* , **82** (1999) 1502.
- [5] FRACHEBOURG L., MARTIN P. A. and PIASECKI J., *Physica A* , **279** (2000) 69.
- [6] RAMAN C. V., *Phys. Rev.* , **12** (1918) 442.
- [7] BRILLIANTOV N. and PÖSCHEL T., *Kinetic theory of granular gases* (Oxford University Press, New York) 2004.
- [8] SINDE M., DAS D. and RAJESH R., *Phys. Rev. Lett.* , **99** (2007) 234505.
- [9] BEN-NAIM E., CHEN S. Y., DOOLENAND G. D. and REDNER S., *Phys. Rev. Lett.* , **83** (1999) 4069.
- [10] SHINDE M., DAS D. and RAJESH R., *Phys. Rev. E* , **79** (2009) 021303.
- [11] FRACHEBOURG L. and MARTIN P. A., *J. Fluid. Mech.* , **417** (2000) 323.
- [12] TÄUBER U. C., HOWARD M. and VOLLMAYR-LEE B. P., *J. Phys. A: Math. Gen.* , **38** (2005) R79.
- [13] CARDY J., FALKOVICH G. and GAWEDZK K., *Non-equilibrium Statistical Mechanics and Turbulence* (Cambridge Univ. Press, Cambridge) 2008.
- [14] WIJLAND F. v., *Phys. Rev. E* , **63** (2001) 022101.
- [15] BALDASSARRI A., MARCONI U. M. B. and PUGLISI A., *Advances in Complex Systems* , **4** (2001) 321.
- [16] BALDASSARRI A., MARCONI U. M. B. and PUGLISI A., *Europhys. Lett.* , **58** (2002) 14.
- [17] MARCONI U. M. B., BALDASSARRI A. and PUGLISI A., *Phys. Rev. E* , **65** (2002) 051301.
- [18] BEN-NAIM E. and KRAPIVSKY P. L., *Lecture Notes in Physics* , **624** (2003) 65.
- [19] OSTOJIC S., PANJA D. and NIENHUIS B., *Phys. Rev. E* , **69** (2004) 041301.
- [20] BORTZ A. B., KALOS M. H. and LEBOWITZ J. L., *J. Comp. Phys.* , **17** (1975) 10 .
- [21] GILLESPIE D. T., *J. Comp. Phys.* , **22** (1976) 403.
- [22] GILLESPIE D. T., *J. Phys. Chem.* , **81** (1977) 2340.
- [23] GILLESPIE D. T., *Annu. Rev. Phys. Chem.* , **58** (2007) 35.
- [24] ARFKEN G. B. and WEBER H. J., *Mathematical Methods for Physicists* (Elsevier Academic Press, California) 2005.

- [25] BARRAT A., BIBEN T., RCZ Z., TRIZAC E. and VAN WIJLAND F., *Journal of Physics A: Mathematical and General*, **35** (2002) 463.
- [26] BRAY A. J., *Adv. Phys.*, **43** (1994) 357.